High-Speed 1x16 Optical Switch Monolithically Integrated on InP

I. M. Soganci[(1)], T. Tanemura[(1)], K. A. Williams[(2)], N. Calabretta[(2)], T. de Vries[(2)], E. Smalbrugge[(2)], M. K. Smit[(2)], H. J. S. Dorren[(2)], and Y. Nakano[(1)]

[(1)] Research Center for Advanced Science and Technology, University of Tokyo, Tokyo, Japan, imsoganci@hotaka.t.u-tokyo.ac.jp
[(2)] COBRA Research Institute, Eindhoven University of Technology, Eindhoven, the Netherlands

Abstract We present the first fully integrated high-speed 1x16 InP optical switch based on arrayed phase modulators, demonstrating average extinction ratio of 17.0 dB, estimated on-chip loss of <8 dB, and reconfiguration time of <6 ns.

Introduction

In ultra-high-bit-rate optical communication networks, transparent optical packet switching (OPS) may offer significant reduction of power consumption and cost compared to electronic switching[1]. The throughput of routers, which is estimated to be close to 1 Pbit/s by 2020[2], necessitates the OPS nodes to have large number of ports as well as nanoseconds or shorter dynamic response time. In particular, wavelength-independent broadband switching is attractive to fully utilize the transparency of data format and bit-rate as well as ultra-short latency of OPS. To achieve such large-scale, high-speed, and wavelength-independent switches, those based on III-V semiconductor can be advantageous in terms of integrability with other active and passive devices, small footprint and power consumption[3,4].

In this paper, we realize, for the first time, a monolithically integrated InP 1x16 optical switch based on arrayed phase modulators. We experimentally demonstrate switching to all 16 output ports with average extinction ratio of 17.0 dB and the reconfiguration time below 6 ns. To our knowledge, this is the largest-scale high-speed monolithically integrated semiconductor optical switch ever reported, in terms of the number of output ports.

Design and fabrication of the device

The principle of operation of the integrated optical phased-array switch has been explained in our previous publications[5,6]. The device consists of two free propagation regions, an array of waveguides with phase modulators, a passive input waveguide and an array of passive output waveguides. The design is shown in the schematic diagram in Fig. 1. When linear phase distribution is maintained in the arrayed waveguides, constructive interference occurs at a number of points separated by the free spectral range at the output plane. The location of these points is a linear function of the phase difference between the adjacent arrayed waveguides. The phase conditions at the arrayed waveguides, thus the output port to be on, can be controlled dynamically through the phase modulator array.

The dimensions of the star couplers, waveguide width, depth and pitch of the waveguides at the array and output planes must be calculated carefully for optimal operating conditions. In this particular device, we use shallowly etched InP/InGaAsP ridge waveguides in the entire device, with InP/InGaAsP p-i-n double heterojunction epitaxial structure. The phase modulation is achieved through both the reverse-biasing (electo-optic effect) and forward-biasing (carrier effect). The waveguide width is set to 3.5 μm at the phase-modulators and 2 μm elsewhere. The minimal radius of curvature in the waveguide bends is 500 μm. The number of phase modulators is chosen to be 24, which is close to the optimal value according to our calculations[7]. The total length of the device is 4.5 mm. The footprint can be further minimized if waveguides with higher refractive index contrast are used, which decreases both the radius of curvature and the length of the star couplers.

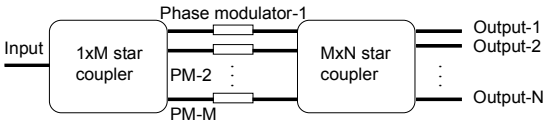

Fig. 1: Schematic of the integrated optical phased-array switch

Single-step metal-organic vapour phase epitaxy (MOVPE) was used for the growth of the wafer. Ridge waveguides were formed by double-step reactive ion etching (RIE) down to the top of the guiding layer. The highly doped InGaAs contact layer was removed from the top of the passive waveguides to decrease the propagation loss. Passive waveguides were isolated from electrical connection by using polyimide and a thick layer of photoresist. The electrodes were formed by electron-beam evaporation of Ti, Pt and Au and lift-off. The fabricated sample was cleaved into individual switches and bonded on thermally conductive AlN submounts. The electrode pads were wire-bonded to the submount. The optical microscope image of the fabricated 1x16 switch is displayed in Fig. 2.

Experimental characteristics

Basic static and dynamic characteristics of the optical switch were measured with TE-polarized continuous-wave output of a laser diode at 1.55-μm wavelength. The light was coupled to the input and from the output waveguides of the switch using lensed optical fibres.

978-3-8007-3173-2

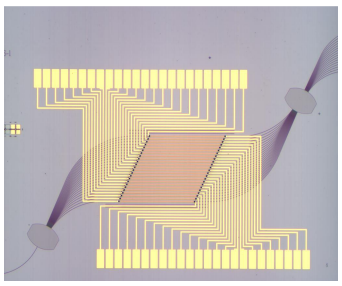

Fig. 2: Optical microscope image of the integrated 1x16 optical phased-array switch (4.5 mm x 3.1 mm)

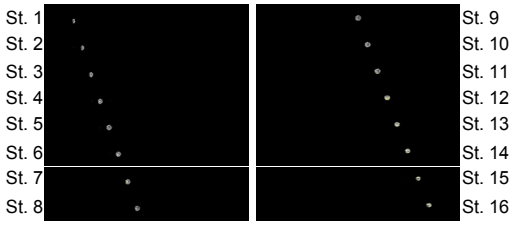

Fig. 3: Near-field images at the output facet of the optical switch observed at different states (St. 1-St. 16).

Microscope lenses and an infrared camera were also used to view the near-field images at the output plane.

During the static measurements, the phase modulators were controlled by DC voltages from 24 channels of power supplies. The voltages at all phase modulators were optimized in the range from -10 V to +1.5 V, so that the optical power coupled from the corresponding output port was maximized at each of the 16 states. Figure 3 shows the near-field images captured by an infrared camera at the output facet at 16 different states of the switch.

We measured the optical power coupled from the output ports to the optical fibre at all states to observe the extinction and crosstalk characteristics. In Fig. 4, the normalized optical power values at all ports are compared in each state. The average crosstalk suppression ratio is 17.0 dB and the extinction ratio is higher than 9.4 dB at all outputs. These values are smaller than the analytically calculated ones, probably because of electrical crosstalks between some of the phase modulators, which were not isolated sufficiently, and the not perfectly optimized iterative algorithm we used in the experiment. The non-uniformity of power between on outputs is less than 4.2 dB. We measured the fibre-to-fibre loss of the on outputs as between 14.7 dB and 18.9 dB. Assuming that the fibre-to-waveguide coupling loss is approximately 5-6 dB for the used polarization and wavelength, the on-chip loss is estimated to be in the 4-8 dB range.

Finally, we measured the reconfiguration time of the switch by sending a square-wave signal to one of the phase modulators and monitoring the optical power at the output using a high-speed photodetector and a digital sampling oscilloscope. Fig. 5 shows the observed transient waveform. The 10-90 % rise and fall times are measured to be less than 6 ns. Although this is a simplified measurement with only one

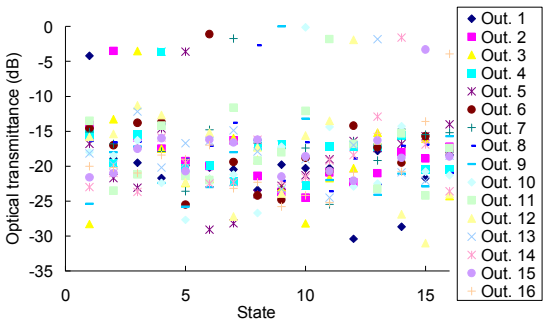

Fig. 4: Normalized optical power (dB) at the outputs of the switch at all 16 states.

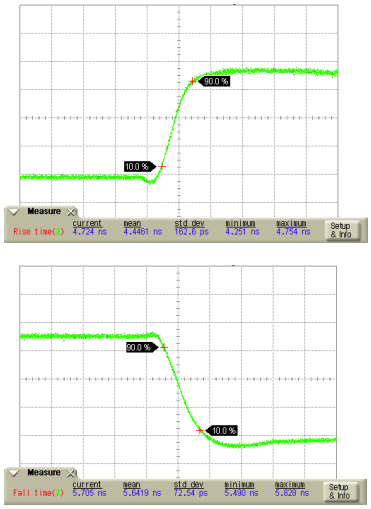

Fig. 5: Dynamic switching responses observed at the rise time (top) and fall time (bottom). (5ns/div)

electrode driven dynamically, complete dynamic switching below 6 ns should be possible if we could drive all the 24 electrodes synchronously.

Conclusions

We have fabricated and experimentally demonstrated a monolithically integrated InP 1x16 optical switch for the first time. The average extinction ratio of 17.0 dB, estimated on-chip optical loss of less than 8 dB, and dynamic response time below 6 ns were obtained. Moreover, the switch should operate independent on the signal wavelength[6]. These results show the potential of phased-array scheme in realizing large-scale ultra-broadband optical packet switches in the future photonic network.

References

1 S. J. B. Yoo, J. Lightwave Technol. 24, 4468 (2006).
2 R. S. Tucker, J. Lightwave Technol. 24, 4655 (2006).
3 K. A. Williams, et al., IEEE J. Sel. Top. Quantum Electron., 11, 78 (2005).
4 Y. Kai, et al., Proc. ECOC'08, We.2.D.4 (2008).
5 T. Tanemura et al., IEEE Photon. Technol. Lett. 20, 1063 (2008).
6 I. M. Soganci et al., Proc. OFC'09, OWV1 (2009).
7 T. Tanemura et al., IEICE Electron. Express, 5, 603 (2008).